JOURNAL OF MATERIALS SCIENCE 28 (1993) 4273–4278

Fabrication and characterization of $YBa_2Cu_3O_{7-x}$/Sn composite superconductors

Part III *Sintering at high-temperature*

R. CHAIM, Y. EZER
Department of Materials Engineering, Technion-Israel Institute of Technology, Haifa, 32000 Israel

$YBa_2Cu_3O_{7-x}$/Sn composites containing 5, 10, 15, and 20 wt% Sn were prepared by conventional powder metallurgy and pressureless sintering at 950 °C. Sn caused degradation of the ceramic superconductor by its chemical reaction with Ba, whose extent increased with Sn content. Composites with between 5 and 10 wt% Sn preserved their superconducting critical temperature, T_c, those with higher Sn content exhibited non-zero residual resistivity at low temperatures. Room-temperature resistivity and its thermal coefficient also increased with Sn content. The brittle behaviour of the composites is attributed to oxidation of Sn during sintering.

1. Introduction

Bulk high-temperature ceramic superconductors for engineering applications are best realized in the form of ceramic/metal composites (cermets) [1–6]. Possible advantages of such composites are their improved ductility and enhanced fracture toughness, as well as thermal stability with the metallic phase acting as a local heat sink. In addition, the metallic phase provides an alternative path for electron conduction, an important feature in the event of a local breakdown.

The microstructural aspects of the cermets and effects on their physical properties give rise to three distinct morphologies: (a) an isolated ceramic phase within a continuous metallic/polymeric matrix [1–3]; (b) an isolated metallic phase within a continuous ceramic matrix [4–6]; and (c) the most promising microstructure, with both the ceramic and the metallic phases spatially continuous.

$YBa_2Cu_3O_{7-x}$/Sn composites fabricated by pressureless sintering at 230 °C (Parts I and II [7, 8]) resulted in a microstructure of type a, due to an absence of bonding between the superconductor grains. Higher temperatures enhanced the sinterability of the superconducting phase and resulted in type b microstructures.

This paper describes the microstructural evolution at 950 °C, and its effects on the mechanical and electrical properties of the composites.

2. Experimental procedure

$YBa_2Cu_3O_{7-x}$ (YBCO) powder was prepared by a solid-state reaction of high-purity Y_2O_3, $BaCO_3$ and CuO powders. The preparation procedure is described in detail in Part I [7]. The resulting product, which contained only the orthorhombic phase, was mixed in different proportions with high-purity Sn powder (0, 5, 10, 15, 20 wt% Sn). The mixtures were mechanically mixed for 30 min in air in an agate mortar. Discs 17 mm in diameter and 5 mm thick were cold pressed at 200 MPa, and sintered in air at 950 °C for 2 h.

Optical (polarized light) and scanning electron microscopy (SEM, JSM 840) combined with X-ray energy-dispersive spectroscopy (EDS) were used for microstructural and microchemical analyses. The ceramographic specimens were prepared by dry sectioning and mechanical polishing down to 0.25 μm, using an oil-based diamond spray on nylon cloth. These specimens were used later for Vickers hardness tests, where a 0.3 kg load was applied for a 10 s duration.

Specimens $4 \times 4\ mm^2$ in cross-section and 2 mm thick were cut and used for compressive tests in air, using an Instron machine (Model 1362) with crosshead velocity 50 μm min^{-1}.

X-ray diffraction (XRD) was used to characterize the phase content, using a diffractometer (PW 1820) with monochromatic CuK_α radiation at 40 kV and 40 mA, at a scanning speed of 0.25° min^{-1}.

Rectangular bars of $2 \times 5 \times 15$ mm were dry cut from the discs for electrical-resistivity measurements. A four-probe technique was applied, with the set-up shown in Fig. 1 of Part II [8], using a 10 mA direct current via a programmable current source (Keithley model 224) and digital multimeter (Keithley model 196). The temperature was measured with a copper–constantan (type T) thermocouple.

3. Results

3.1. Microstructural characterization

The microstructure of the sintered specimens was often macroscopically inhomogeneous, with a top layer which was more porous than the rest of the

0022–2461 © *1993 Chapman & Hall*

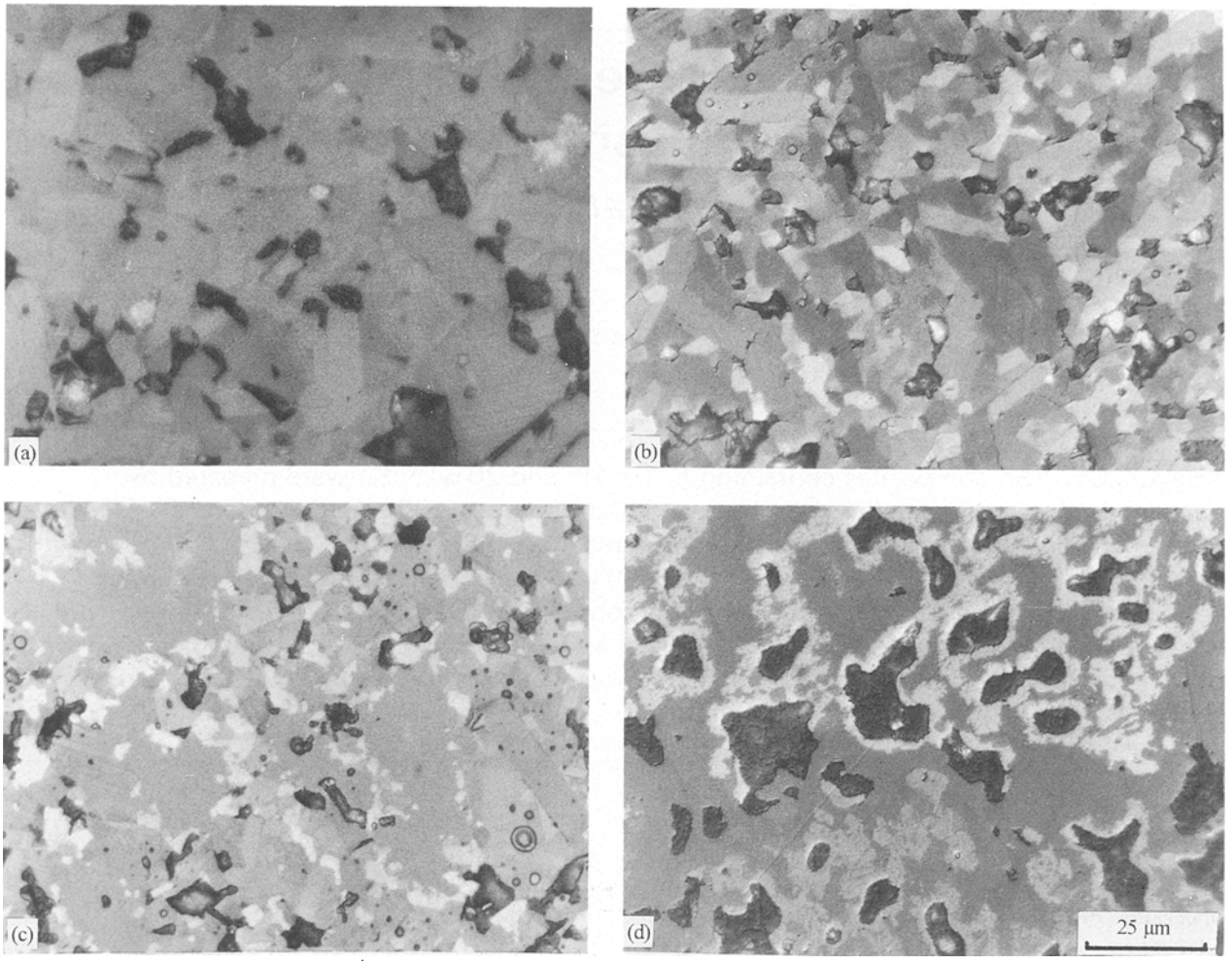

Figure 1 Optical micrographs of $YBa_2Cu_3O_{7-x}$/Sn composites with different Sn contents, sintered at 950 °C for 2 h: (a) pure YBCO, the internally twinned orthorhombic phase dissociates into the x-phase as well as into $BaSnO_3$ and CuO with an increase in Sn content (wt %); (b) 5 wt %; (c) 10 wt %; (d) 20 wt %.

specimen and which was 25% of the thickness. This microstructure may be due to gravity segregation of the Sn at elevated temperatures. For all measurements the denser sections of the specimens were characterized after removal of this upper layer.

The multiphase nature of the various composite specimens was confirmed under polarized light, as shown in Fig. 1. The pure YBCO specimen exhibited internally twinned grains–typical for the orthorhombic phase (Fig. 1a) – as well as some porosity. In the 5 and 10 wt % Sn variants, additional phases were observed (Figs 1b, c), differing in optical activity but with the same degree of porosity. By contrast, the 15 and 20 wt % Sn variants were basically free of the superconducting phase, their distinct microstructure consisted of large grains of a constituent designated as the x-phase, whose formation was enhanced by an increase of the Sn content and accompanied by higher specimen porosity (Fig. 1d). The x-phase often had a core of tin oxide (Fig. 2a) and was covered by a layer of CuO (Fig. 2b), as was confirmed both by EDS microanalysis and XRD. These findings indicate that the x-phase may be the product of oxidation/reduction reactions between SnO_2 and YBCO. EDS composition analysis determined its average composition as $BaSn_{0.8}Y_{0.12}CuO_x$. Barium stannate ($BaSnO_3$) was formed at the same time.

XRD spectra for the various specimens are shown in Fig. 3, from which decomposition of YBCO and formation of the x-phase, $BaSnO_3$ and CuO were deduced. XRD results also indicated the presence of $BaCuO_2$ (1 1 2 phase) as a minor constituent (less than 5 vol %) in specimens with Sn content above 10 wt %. No metallic Sn survived these sintering heat treatments.

3.2. Electrical properties

The variation of electrical resistivity of the various specimens with temperature is shown in Fig. 4. Both room-temperature and low-temperature ($T = 100$ K) resistivity increased by an order of magnitude at each 5 wt % Sn increment up to the 10 wt % level (Fig. 4a, b, c). A similar trend was observed for the corresponding temperature coefficients, $\alpha = d\rho/dT$; see the caption to Fig. 4.

While the 5 and 10 wt % Sn variants preserved their superconducting-transition temperature, T_c, at around 92 K, which is similar to that of pure YBCO, those with higher Sn content exhibited a significant drop in resistivity (albeit not to zero) near the original transition temperature (Fig. 4d). The transition interval, ΔT_c widened from 2 K in pure YBCO to about 14 K in the 15 wt % Sn specimen.

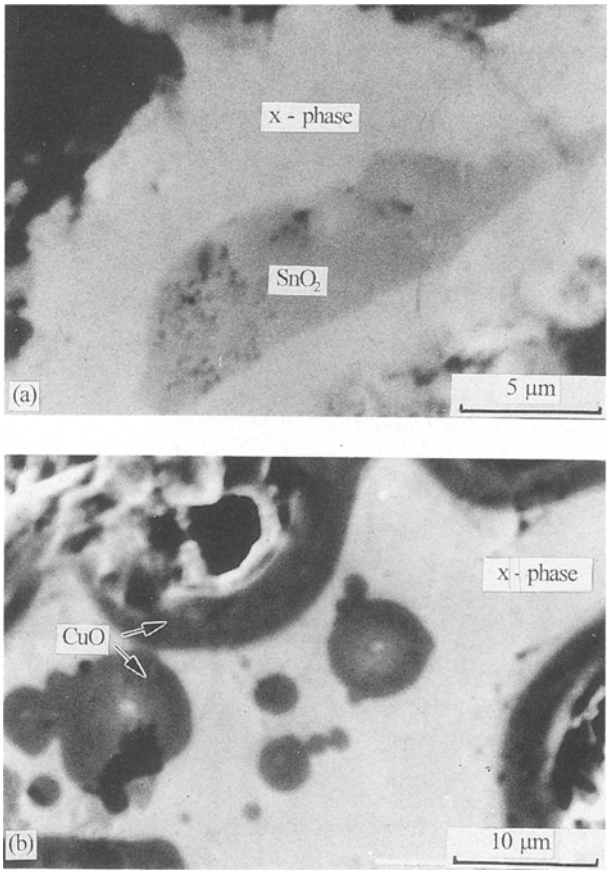

Figure 2 SEM images of the SnO_2 core surrounded by $Y_{0.12}BaSn_{0.8}CuO_x$ and CuO layers: (a) 5 wt % Sn, and (b) 20 wt % Sn.

3.3. Mechanical properties

The dense regions of the 5 and 10 wt% Sn variants and pure YBCO specimens were tested in compression. Typical stress–strain curves are shown in Fig. 5. In contrast to the brittle behaviour of the pure compound, the multiphase specimens exhibited some residual strength after failure (Fig. 5) – a possible indication that the x-phase has higher strength and stiffness than YBCO, and exerts a toughening effect. The increase in average compressive strength with Sn content (Fig. 6) is also compatible with a higher strength of the x-phase, even though the increase in the porosity was not allowed for. No meaningful changes in hardness were observed (Fig. 7).

4. Discussion

In Parts I and II [7, 8], carried out at 230 °C, no interaction occurred between the two components. However, sintering around the 950 °C level is expected to promote chemical reactions in the system. Linear extrapolation of the diffusion-coefficient data of Sn in YBCO [9], assuming no anomalies, yields a value of approximately 2×10^{-10} $m^2 s^{-1}$ for 950 °C – a value comparable to the approximate diffusion distance of 1200 μm (far beyond the average YBCO-grain size) and a possible explanation for the extensive reactions observed between the metal, its oxides and YBCO.

Increase of the sintering temperature to 950 °C is accompanied by rapid oxidation of the metallic Sn pockets, both by atmospheric oxygen and by reduction of YBCO. At low Sn contents (5 and 10 wt %), the scope of this reaction is limited and permits sintering to take place without detriment to the 1–2–3 stoichiometry of the YBCO phase. As the Sn content increases, more "liquid pockets" become available in the matrix, thus promoting decomposition of the YBCO grains.

EDS microanalyses of the 5 wt % and 20 wt % Sn specimens by SEM in conjunction with the XRD results were used to characterize the reactions between YBCO and Sn. Dissolution of oxygen in tin was reported [10] to lower the surface tension, with an attendant favourable effect on wettability. It appears that Sn particles undergo oxidation when heated above their melting point. Oxidation of Sn at the boundaries of YBCO grains destabilizes the grains by preferential dissolution of barium in the reaction product. The resulting $BaSnO_3$ phase is extremely stable and was reported to form readily in other similar systems [11]. In addition, reduction of the YBCO grains by loss of oxygen to Sn at high temperatures was proved by X-ray photoelectron spectroscopy (XPS) [12] and is associated with formation of CuO. The final product is the x-phase.

Alloying of YBCO with Sn [13–15] and SnO_2 [16, 17] indicated that the critical temperature, T_c, may be preserved at low percentages of SnO_2 (10 wt % Sn, 5 mol % SnO_2). The limited solubility of Sn in YBCO is most probably due to its ionic radius (0.069 nm for Sn^{4+}) [18], which makes it suitable as a substituent ion for Cu^{2+} (0.071 nm) [18] in YBCO. Nevertheless, some investigations [11, 16] report precipitation of the second phase at high temperatures.

The observed increase in electrical resistivity with Sn content is associated with the electrically insulating nature of the x-phase, as well as with the contribution of the porosities. The corresponding increase in the thermal coefficient, α, is compatible with formation of non-conducting interfacial phases like CuO between the YBCO grains.

The widening of the superconducting-transition interval with increases in Sn content is in agreement with resistivity measurements reported for substitution of Sn for Cu in $DyBa_2Cu_3O_{7-x}$ [11]. These changes, together with the drop in T_c, become substantial only beyond 25 vol % Sn, and further increases in Sn content are expected to lead to semiconducting behaviour in the normal state.

As regards the mechanical properties, the anomalous stress–strain behaviour and the increase in compressive strength with Sn content are both attributable to the multiphase microstructure, in which the component phases exhibit different stiffness characteristics.

Acknowledgements

The authors acknowledge the Sachs Center at the Department of Materials Engineering for providing the facilities used for this study. Partial financial support by the Fund for the Promotion of Research at the Technion is also acknowledged.

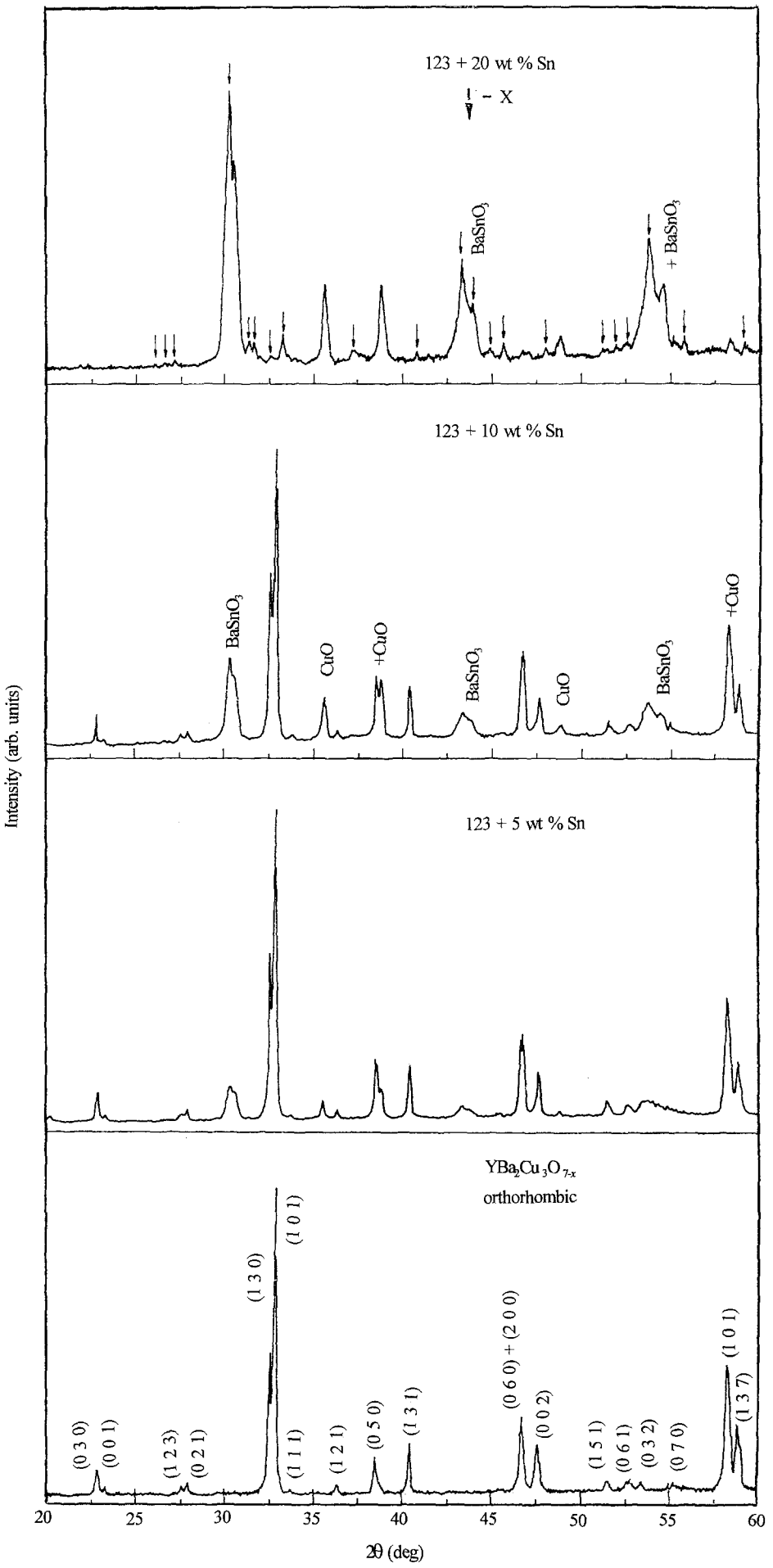

Figure 3 XRD spectra of $YBa_2Cu_3O_{7-x}$/Sn composites with different Sn contents, showing the dissociation of YBCO and the formation of $BaSnO_3$ and the x-phase.

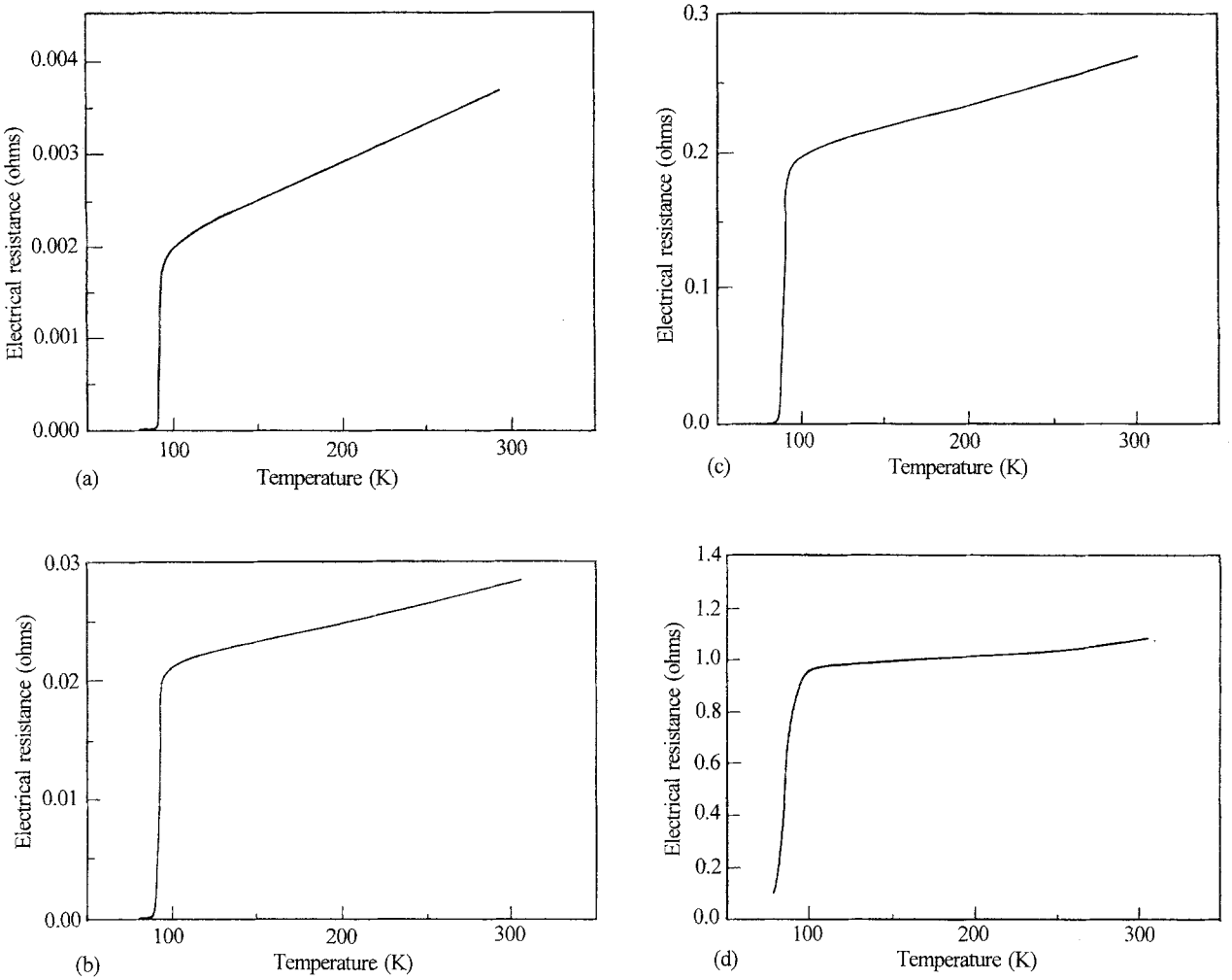

Figure 4 Electrical resistivity of $YBa_2Cu_3O_{7-x}$/Sn multiphase specimens versus temperature: (a) pure YBCO, $\alpha = 8.3 \times 10^{-8}\ \Omega\,m\,K^{-1}$; (b) 5 wt % Sn, $\alpha = 3.2 \times 10^{-7}\ \Omega\,m\,K^{-1}$; (c) 10 wt % Sn, $\alpha = 3.2 \times 10^{-6}\ \Omega\,m\,K^{-1}$; and (d) 15 wt % Sn, $\alpha = 5.2 \times 10^{-6}\ \Omega\,m\,K^{-1}$.

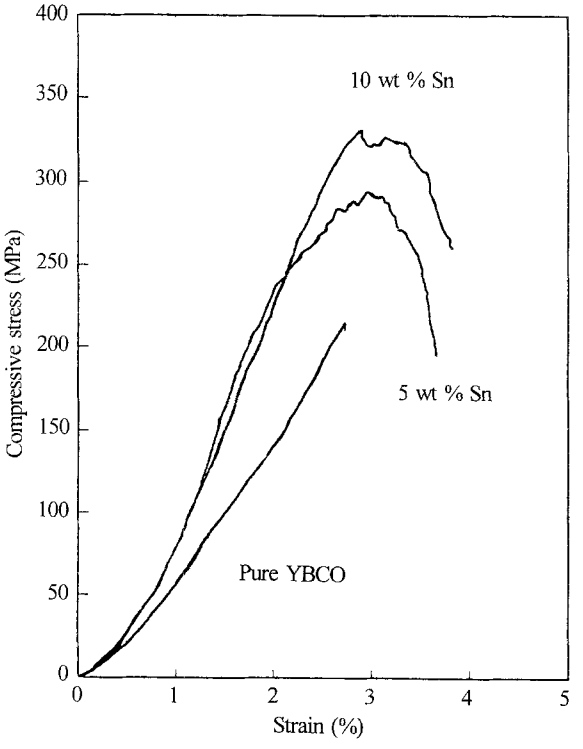

Figure 5 Characteristic compressive stress–strain curves of: pure YBCO, $YBa_2Cu_3O_{7-x}$/Sn–5 wt %, and $YBa_2Cu_3O_{7-x}$/Sn–10 wt % specimen.

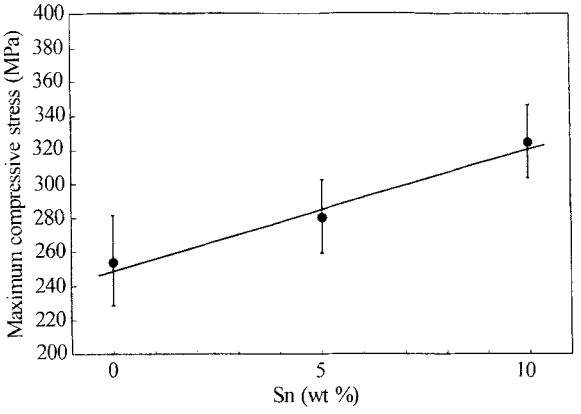

Figure 6 Maximum compressive strength versus Sn content.

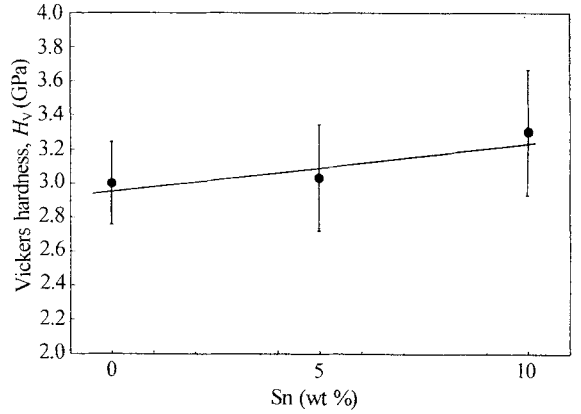

Figure 7 Vickers hardness versus Sn content.

References

1. C. W. NIES, B. E. SMITH, J. M. NICKEL, W. W. CAO, T. T. SRINIVASAN, A. S. BHALLA, R. E. NEWNHAM, and L. E. CROSS, *Mater. Res. Bull.* **23** (1988) 623.
2. A. GOYAL, P. D. FUNKENBUSCH, G. C. S. CHANG, and S. J. BURNS, in "Superconductivity and its applications", edited by H. S. Kwok and D. T. Shaw (Elsevier, Buffalo, NY, 1988) p. 223.
3. H. V. NGUYEN, T. T. SRINIVASAN, R. E. NEWNHAM, and A. S. BHALLA, *J. Mater. Sci. Mater. Elec.* **2** (1991) 177.
4. L. S. YEOU and K. W. WHITE, *J. Mater. Res.* 7 (1992) 1.
5. J. J. LIN, T-M. CHEN, Y. D. YAO, J. W. CHEN, and Y. S. GOU, *Jpn. J. Appl. Phys.* **29** (1990) 497.
6. P. U. D. MURALIDHARAN, K. V. PAULOSE, J. KOSHY, and A. D. DAMODARAN, *J. Am. Ceram. Soc.* **74** (1991) 2679.
7. R. CHAIM and Y. EZER, *J. Mater. Sci.* **28** (1993).
8. *Idem, ibid.* **28** (1993).
9. V. N. ALFEEV, P. P. GORBIK, V. V. DYAKIN, F. A. ZAITOV, V. M. OGENKO and G. M. SHALYAPINA, *Solid State Comm.* **77** (1991) 49.
10. A. PASSERONE, E. RICCI and R. SANGIORGI, *J. Mater. Sci.* **25** (1990) 4266.
11. C. WANG, L. T. CHEN, H. L. CHANG, M. L. CHU, F. W. HSU, T. M. CHEN, T. J. YANG, Y. S. GOU and T. M. UEN, *Jpn. J. Appl. Phys.* **28** (1989) 2459.
12. Y. SUZUKI, T. KUSAKA, A. AOKI, T. AOYAMA, T. YOTSUYA and S. OGAWA, *Jpn. J. Appl. Phys.* **28** (1989) 2463.
13. Y. MAENO, M. KATO, Y. AOKI, T. NOJIMA and T. FUJITA, *Physica B* **148** (1987) 357.
14. T. YUEN, C. L. LIN, J. E. CROW, G. N. MYER, R. E. SALMON, P. SCHLOTTMANN, N. BYKOVETZ and W. N. HERMAN, *Phys. Rev. B* **37** (1988) 3770.
15. C. S. PANDE, H. A. HOFF, A. K. SINGH, M. S. OSOFSKY, M. A. IMAM, K. SADANANDA and L. E. RICHARDS, *IEEE Trans. Magnet.* **25** (1989) 2004.
16. T. SUZUKI, T. YAMAZAKI, A. KOUKITU, M. MAEDA, H. SEKI and K. TAKAHASHI, *J. Mater. Sci. Lett.* **7** (1988) 926.
17. T. SUZUKI, T. YAMAZAKI, R. SEKINE, A. KOUKITU, H. SEKI and K. TAKAHASHI, *J. Mater. Sci. Lett.* **8** (1989) 1271.
18. R. D. SHANNON, *Acta Cryst. A* **32** (1976) 751.

Received 3 November
and accepted 19 November 1992